

# Determination of the possible magnitude of the charging effect in a SCALPEL mask membrane

M. M. Mkrtchyan,<sup>a)</sup> A. S. Gasparian, K. A. Mkhoyan, J. A. Liddle, and A. E. Novembre  
*Bell Laboratories of Lucent Technologies, Murray Hill, New Jersey 07974*

(Received 3 June 1999; accepted 10 September 1999)

Previously, we theoretically investigated the charging of free standing dielectric thin films irradiated by 100 keV electrons and formulated kinetic equations describing the dynamic process [M. Mkrtchyan *et al.*, *Microelectron. Eng.* **46**, 233 (1999)]. It was shown that in the currently used SCALPEL® masks comprising a 1000-Å-thick amorphous SiN<sub>x</sub> film supported by a grillage of Si struts, the membrane charging could be significant and might have an adverse effect on the system performance. The membrane charging, sensitive to both the conductivity and the geometry of conductive path, can be regulated in a straightforward manner by tailoring both of them; for instance, by applying a top surface conductive layer (TSCL) with an appropriate thickness and doping level. Here we discuss the results obtained on the basis of our charging model modified to be applicable to the case of a SiN<sub>x</sub> membrane with a TSCL (e.g., a 10-nm-thick amorphous Si or poly-Si film doped by boron). The results presented demonstrate that this modification of the membrane is sufficient to avoid the adverse effect of the mask-membrane charging. The required structure can be generated simply by regulating the gas flows in the low-pressure chemical vapor deposition process to produce a thin final layer of *a*:Si or poly-Si which can be doped during or after deposition. © 1999 American Vacuum Society. [S0734-211X(99)12406-5]

## I. INTRODUCTION

Charging of SCALPEL mask membranes can have an adverse effect on the system performance. It creates an electrostatic field in the membrane that deflects the incident electrons while they travel through the mask membrane. The current SCALPEL masks consist of a thin SiN<sub>x</sub> film supported by a silicon grillage<sup>1</sup> (Figs. 1 and 2). The latter can be grounded to provide a conductive path for the electrostatic charge accumulated in the insulating film during the electron irradiation.

Our investigation has shown that SiN<sub>x</sub> mask-membrane charging is mostly due to the limited conductivity of the membrane dielectric material, the small cross section of the conductive path [defined by the membrane thickness (normally 750–1500 Å)], and the existence of a high density of trapping centers for the charge carriers.<sup>2</sup> Because the trapping centers are uniformly distributed throughout the membrane, the charge accumulated in the membrane will be distributed uniformly as well, giving rise to a nonuniform distribution of the electrostatic field, **E**, inside the membrane volume exposed by the electron beam; **E** will be zero in the center and maximal at the edges of the subfield and at the membrane surfaces. Depending on the exposure dose, the electrostatic field can cause either image placement errors (for low doses) or illumination nonuniformities (for high doses) on the wafer across the scan stripe (Sec. III).<sup>1</sup>

Recently we have investigated the charging and radiation damage effects that occur when a free standing thin dielectric film is exposed to constant irradiation by energetic electrons.<sup>1–3</sup> We have measured electron energy loss spectra of 100 keV electrons transmitted through the SiN<sub>x</sub> films

and have performed accelerated lifetime radiation testing using a scanning transmission electron microscope (STEM) equipped with a high-brightness cold field-emission gun.<sup>3</sup> These results were used as a supplement to the theoretical investigation of the processes responsible for the charging in free standing dielectric thin films. We have developed a comprehensive model of the electrostatic charge accumulation in free standing dielectric films supported by a Si grillage and have formulated kinetic equations describing the dynamic process.<sup>1,2</sup>

The film charging effect is sensitive to many factors such as the material electrical characteristics, its electronic structure, and the sample geometry; for instance, film thickness change might change not only the quantity but also the sign of the accumulated charge and related surface potential.<sup>4</sup> In this article we have extended our model<sup>1–3</sup> to analyze the charging effect of the SCALPEL mask membranes with a TSCL (Fig. 1). The simulation results presented here demonstrate that a simple modification of the mask membrane deposition process (Sec. IV) can dramatically suppress the adverse effect of membrane charging on the image quality in a SCALPEL system.

## II. CHARGING OF SiN<sub>x</sub> MEMBRANES WITH TSCL

The variety of processes responsible for the charging of free standing *a*:SiN<sub>x</sub> thin films irradiated by 100 keV electrons has been discussed elsewhere.<sup>1,2</sup> The mechanism for the charging of free standing dielectric films irradiated by the fast electrons is shown in Fig. 2.<sup>2</sup> This mechanism still applies when a TSCL is used on top of the basic dielectric membrane because the thickness of the boron doped silicon TSCL is expected to be much smaller than the mean free path for the dominant charge carrier generation process,  $\Lambda$ .

<sup>a)</sup>Electronic mail: masis@lucent.com

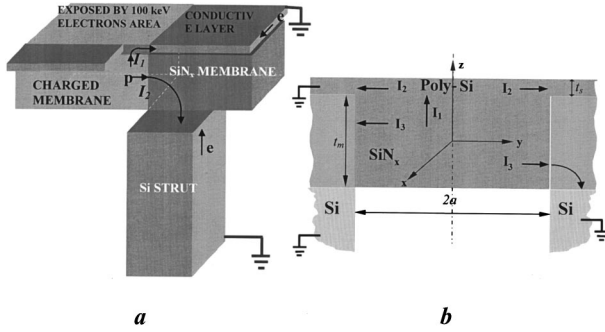


FIG. 1. Structure and charge transport schematics for a SCALPEL  $\text{SiN}_x$  mask membrane supported by the Si struts when a TSCL is applied on top of the membrane; (a) general view, (b) cross section of the exposed region of the membrane stack and hole fluxes responsible for the charge transport. Vertical scale is exaggerated to make demonstration of details possible.

This process originates from the decay of plasmons generated by the incident electrons<sup>1,2</sup> which have a  $\Lambda_p > \Lambda$  of about 110 nm in the case of  $\text{SiN}_x$  membrane irradiated by 100 keV electrons.<sup>2</sup>

The kinetic equations describing the dynamics of the charging effect need to be modified to account for the existence of a TSCL with a conductivity much higher than the conductivity of the basic membrane supported by Si struts.

According to the charging mechanism presented in Fig. 2, the dielectric membrane will be positively charged generating an electrostatic field that is symmetric to the center of the exposure field.<sup>2</sup> The electrostatic field will force mobile holes out of the membrane exposed area. The cross section of the exposed region of the membrane stack ( $\text{SiN}_x$  + TSCL) supported by Si struts is schematically shown in Fig. 1(b). Accordingly, one needs to consider three fluxes of mobile holes; (i) the flux from  $\text{SiN}_x$  into the top conductive layer,  $I_1$ , driven by the  $E_z$  component of the electrostatic field, (ii) the flux driven by  $E_y$  in the TSCL,  $I_2$ , parallel to the membrane surface, and (iii) the flux through the edge of the membrane,  $I_3$ , again due to  $E_y$  [Fig. 1(b)].

The hole current in different regions,  $I_i$ , is proportional to the electrostatic field strength,  $E_i$ , the effective cross section of the hole conductive path,  $A_i$ , in the particular region, and the conductivity of the material,  $\sigma_i = e\mu_i N_i$ , in that region defined by the hole mobility,  $\mu_i$ , and density,  $N_i$ ,

$$I_i = \sigma_i \langle E_i \rangle A_i. \quad (2.1)$$

Here  $\langle E_i \rangle$  is the electrostatic field supporting the hole flux in the  $i$ th region averaged over the effective cross section of the corresponding conductive path;  $E_1 \equiv E_z - \text{SiN}_x$ ,  $E_2 \equiv E_y - \text{Si}$ , and  $E_3 \equiv E_y - \text{SiN}_x$ .

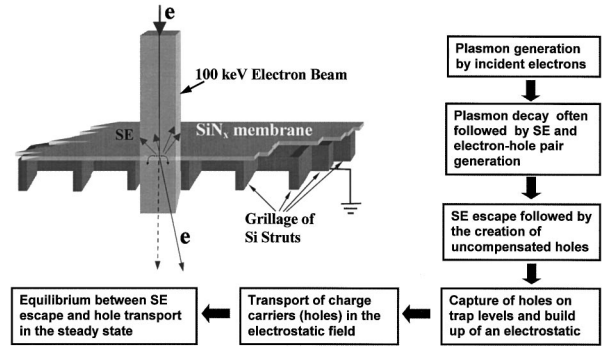


FIG. 2. Schematic view of a SCALPEL mask blank irradiated by the flux of fast electrons and the mask-membrane charging mechanism (see Ref. 2).

In Table I, the expressions and values of all parameters involved are summarized. The strength of the electrostatic field,  $E_i$ , is presented in units of  $E_Q = Q/(2\pi\epsilon_0 A_1)$  where  $Q$  is the total charge accumulated in the membrane volume,  $V = A_1 t_m$ , exposed by the electron beam and  $\epsilon_0$  is the permittivity of the free space. In the expressions presented in Table I,  $p$  is the density of mobile holes,  $N_d$  is the hole density in B-doped poly-Si,  $N_{t2}$  is the density of hole shallow trap levels in  $\text{SiN}_x$ ,  $\chi N_{t2}$  is the fraction of trapped holes thermally released into the valence band<sup>1,2</sup> contributing to the hopping conductivity<sup>5</sup> (see below). Finally,  $F_z(t_m)$  and  $F_y(t_m)$  are weak functions of the membrane thickness ( $\approx 7$  and  $\approx 20$ , respectively) obtained from the numerical calculation of integrals representing  $E_y$  and  $E_z$  [see Eqs. (5.2) and (5.3) in Ref. 2].

It is assumed that the accumulated electrostatic charge is distributed uniformly throughout the  $\text{SiN}_x$  membrane in accordance with the uniform distribution of the hole trap levels.<sup>1,2</sup> Previously, we have calculated the electrostatic field of a uniformly charged  $\text{SiN}_x$  dielectric membrane.<sup>2</sup> In the case considered here, a thin conductive surface layer is added on top of  $\text{SiN}_x$ . Thus, the electrostatic field will be defined by the solution of the Poisson equation for the multilayer stack shown in Fig. 1(b) with boundary conditions at the three interfaces. The problem can be simplified by taking into account the fact that the relative dielectric constants of Si and  $\text{SiN}_x$  are close (10 and 7 correspondingly<sup>6,7</sup>) and, in the first approximation, one can use our previous results obtained for  $\text{SiN}_x$  films [Ref. 2, Eqs. (5.1) and (5.2)] correcting them to account for the small jump of the normal component of the field,  $E_z$ , at the Si/ $\text{SiN}_x$  boundary;  $\epsilon_{\text{Si}} E_{z-\text{Si}} = \epsilon_{\text{SiN}_x} E_{z-\text{SiN}_x}$ .

The total charge escaping from the exposed area of the

TABLE I. Charge carrier density,  $N_i$ , drift mobility,  $\mu_i$ , conductive path cross section,  $A_i$ , and the average electrostatic field,  $\langle E_i \rangle$ , in the different regions with hole fluxes shown in Fig. 1(a).

$i$	Region	$A_i$	$N_i$	$\langle E_i \rangle$	$\mu_i$ (m <sup>2</sup> /V s)	$\sigma_i = e\mu_i N_i$
1	$\text{SiN}_x$	$4a^2$	$(p + \chi N_{t2})$	$E_Q F_z / [(1 + \epsilon_{\text{SiN}_x}) \epsilon_{\text{SiN}_x}]$	$5.0 \times 10^{-6}$	$\sigma_{\text{SiN}_x} = e(p + \chi N_{t2}) \mu_{\text{SiN}_x}$
2	Poly-Si	$2at_s$	$N_d$	$E_Q F_y / (1 + \epsilon_{\text{Si}})$	$10^{-3} \rightarrow 10^{-2}$	$\sigma_{\text{Si}} = e\mu_{\text{Si}} N_d$
3	$\text{SiN}_x$	$2at_m$	$(p + \chi N_{t2})$	$E_Q F_y / (1 + \epsilon_{\text{SiN}_x})$	$5.0 \times 10^{-6}$	$\sigma_{\text{SiN}_x} = e(p + \chi N_{t2}) \mu_{\text{SiN}_x}$

membrane per second in this case is the sum  $I_1 + 2I_3$ , with  $I_1$  and  $I_3$  given as follows:<sup>1,2</sup>

$$I_1 = \sigma_1 \langle E_1 \rangle A_1 \approx e E_Q A_1 F_z(t_m) \chi N_{t2} \mu_{\text{SiN}_x} [(I + \epsilon_{\text{SiN}_x}) \epsilon_{\text{SiN}_x}]^{-1} \\ = (e/\tau_Q) F_z(t_m) / (1 + \epsilon_{\text{SiN}_x}), \quad (2.2)$$

and

$$I_3 = \sigma_1 \langle E_3 \rangle A_3 \approx e E_Q A_3 F_y(t_m) \chi N_{t2} \mu_{\text{SiN}_x} / \epsilon_{\text{SiN}_x} \\ = (e/\tau_Q) (A_3/A_1) F_y(t_m), \quad (2.3)$$

where

$$\tau_Q = \epsilon_{\text{SiN}_x} [E_Q A_1 \chi N_{t2} \mu_{\text{SiN}_x}]^{-1}. \quad (2.4)$$

In Eqs. (2.2) and (2.3), we account for the fact that the hole transport in  $\text{SiN}_x$  is mostly defined by the so-called hopping conductivity,  $\chi N_{t2} \gg p$ ;<sup>5</sup> this is the result of both the existence of a high density of charge trapping centers in  $a:\text{SiN}_x$  and the high rates for hole capture by trap levels.

From Eqs. (2.2) and (2.3) one can see that  $I_1/(2I_3) = (F_z/2F_y)(A_1/A_3)/(1 + \epsilon_{\text{SiN}_x}) \approx 0.02(2a/t_m)$ . Because  $2a/t_m \approx 10^4 \gg 1$ , the ratio  $I_1/(2I_3) \approx 200 \gg 1$  and, therefore,  $I_3$  will be excluded from further discussion.

The capability of the top conductive layer to transport holes is defined by the flux

$$I_s = 2I_2 = 2\sigma_2 \langle E_2 \rangle A_2 \\ \approx e E_Q A_2 F_y(t_m) N_d \mu_{\text{Si}} / \epsilon_{\text{Si}} \\ = (e/\tau_Q) (A_2/A_1) (N_d/\chi N_{t2}) \\ \times (\mu_{\text{Si}}/\mu_{\text{SiN}_x}) F_y(t_m) (\epsilon_{\text{SiN}_x}/\epsilon_{\text{Si}}), \quad (2.5)$$

where  $\mu_{\text{P-Si}}$  denotes the hole drift mobility in a boron doped poly-Si. Note,  $\mu_{\text{P-Si}}$  is a weak function of the doping level; for moderate doping levels,  $N_d < 10^{24} \text{ m}^{-3}$ ,  $\mu_{\text{P-Si}}$  changes from  $\approx 10^{-3} \text{ m}^2/(\text{V s})$  at  $N_d \approx 10^{22} \text{ m}^{-3}$  to  $\approx 4 \times 10^{-3} \text{ m}^2/(\text{V s})$  at  $N_d \approx 10^{24} \text{ m}^{-3}$ .<sup>7,8</sup>

Using Eqs. (2.2) and (2.5), we can calculate the ratio  $I_s/I_1$ :

$$I_s/I_1 = (A_2/A_1) (N_d/\chi N_{t2}) (F_y/F_z) (1 + \epsilon_{\text{SiN}_x}) \\ \times (\mu_{\text{Si}} \epsilon_{\text{SiN}_x}) / (\mu_{\text{SiN}_x} \epsilon_{\text{Si}}) \\ \approx (I + \epsilon_{\text{SiN}_x}) (t_s/a) (N_d/\chi N_{t2}) (\mu_{\text{Si}}/\mu_{\text{SiN}_x}). \quad (2.6)$$

From this equation we find the minimum doping level  $N_{d-\text{min}}$  (for given  $t_s$ ) necessary to match  $I_s$  with  $I_1$

$$N_{d-\text{min}} \approx \chi N_{t2} (\mu_{\text{SiN}_x}/\mu_{\text{Si}}) (1 + \epsilon_{\text{SiN}_x})^{-1} (a/t_s). \quad (2.7)$$

For  $a = 0.5 \text{ mm}$ ,  $t_s = 10 \text{ nm}$  ( $a/t_s = 5 \times 10^4$ ),  $\chi \approx 10^{-4}$ ,  $N_{t2} \approx 0.25 \times 10^{24} \text{ m}^{-3}$ ,  $\mu_{\text{SiN}_x} = 5 \times 10^{-6} \text{ m}^2/(\text{V s})$  (see Ref. 2) we find  $N_{d-\text{min}} \approx 0.003 N_{t2} \approx 0.75 \times 10^{21} \text{ m}^{-3}$  and  $N_{d-\text{min}} \approx 1.4 N_{t2} \approx 0.4 \times 10^{24} \text{ m}^{-3}$  when the top layer is poly-Si [ $\mu_{\text{P-Si}} \approx 1.0 \times 10^{-3} \text{ m}^2/(\text{V s})$ ]<sup>7,8</sup> or  $a:\text{Si}$  [ $\mu_{a:\text{Si}} \approx 0.2 \times 10^{-5} \text{ m}^2/(\text{V s})$ ]<sup>9</sup> correspondingly. One can see that the lower hole mobility of  $a:\text{Si}$  requires a higher density of holes to suppress membrane charging.

Note that even in the case of a TSCL made of crystalline Si (with hole density about  $1.45 \times 10^{16} \text{ m}^{-3}$ ),<sup>6,7</sup> doping is still necessary to increase hole density to a level comparable with  $N_{d-\text{min}}$ . In practice, amorphous or poly-Si can be doped to a level much higher than  $N_{d-\text{min}}$ <sup>7,8,10</sup> therefore, the favorable situation when  $N_d \gg N_{d-\text{min}}$  and hole transport is limited only by the hole flux in  $\text{SiN}_x$  membrane,  $I_s \gg I_1$ , can be easily reached. In this case, the membrane charging dynamics is defined by the membrane material ( $a:\text{SiN}_x$ ) properties only and, as was shown previously (see Refs. 1 and 2), is described by an exponential dependency on the time (or the dose of exposure  $D = I_0 t/A_1$ )<sup>1,2</sup>

$$q(t) = q_s [1 - \exp(-t/\tau_s)]. \quad (2.8)$$

Here  $q_s = q(t)|_{t \rightarrow \infty}$  is the steady state charge and  $\tau_s$  is a time constant characterizing the charging effect; they are given as follows:

$$q_s = e \delta I_0 / [\zeta_s \mu_{\text{SiN}_x} (p_s + \chi N_{t2})] \approx e \delta I_0 / [\zeta_s \mu_{\text{SiN}_x} \chi N_{t2}], \quad (2.9)$$

$$\tau_s = [(\mu_{\text{SiN}_x} \zeta_s \chi N_{t2}) / (eV)]^{-1}, \quad (2.10)$$

where  $\zeta_s = [e^2 V F_z(t_m)] / [2\pi(1 + \epsilon_{\text{SiN}_x}) \epsilon_0 \epsilon_{\text{SiN}_x}]$ ,  $I_0$  is the incident beam current, and  $\delta$  is the secondary electron yield from both surfaces of the membrane (evaluated<sup>2</sup> to be  $\delta \approx 1.0 \times 10^{-4}$  for the case  $E_0 = 100 \text{ keV}$  and the  $\text{SiN}_x$  membrane of thickness  $t_s = 1000 \text{ \AA}$ ). In Eq. (2.9), again, it is taken into account that  $p_s \ll \chi N_{t2}$  (see Ref. 2).

It is interesting to compare the steady state charging characteristics,  $q_{\infty s}$  and  $\tau_{\infty s}$ , with those obtained for the case of the charging of a  $\text{SiN}_x$  membrane without any TSCL,  $q_{\infty 0}$  and  $\tau_{\infty 0}$ .<sup>1,2</sup> (i) Both the steady state charging and transition time are significantly reduced when a TSCL is applied;  $q_{\infty 0}/q_{\infty s} = [F_z(t_m)/F_y(t_m)](a/t_m) \epsilon_{\text{SiN}_x}^{-1} \approx 250$  and  $\tau_{\infty 0}/\tau_{\infty s} \propto (a/t_m \epsilon_{\text{SiN}_x}) > 10^2$ . (ii) In both cases,  $q_{\infty} \propto I_0$  while  $\tau_{\infty}$  is independent of the beam current,  $I_0$ . (iii) A different dependency on the geometry is found:  $q_{\infty 0} \propto (4at_m^2)^{-1}$ ,  $q_{\infty s} \propto (4a^2t_m)^{-1}$ ,  $\tau_{\infty 0} \propto (2a/t_m)$ , and  $\tau_{\infty s}$  is independent of the membrane stack geometry; this indicates that the charging of a membrane with a TSCL is expected to be less sensitive to changes in membrane thickness.

### III. MASK-MEMBRANE CHARGING EFFECT ON THE SCALPEL IMAGE QUALITY

Though the deflection angle at the mask is expected to be relatively small even in the worst case scenario of charging,<sup>1,2</sup> it is necessary to understand what effect electron deflection in the membrane has on the final image in order to ensure that the effect is within acceptable limits.

The effect of the membrane charging on the image quality of a SCALPEL system can be analyzed and evaluated using a thin lens approximation (for details see Ref. 2). The analysis shows that the deflection of an incident electron occurring above the mask (at an angle  $\Delta\alpha_{\text{above}}$ ) and after the mask (at an angle  $\Delta\alpha_{\text{after}}$ ) might have quite a different effect on the image on the wafer depending on the ratio  $\Delta\alpha/\alpha_0$  where  $\alpha_0$  is the SCALPEL back focal aperture (BFP) size. Incident electron deflection above the mask at an angle  $\Delta\alpha_{\text{above}} < \alpha_0$  will have no effect on the image quality at the wafer because



this electron does not carry any information about a particular feature in the mask. If  $\Delta\alpha > \alpha_0$ , the incident electron will be stopped by the BFP no matter where it was deflected; this might cause across subfield illumination nonuniformity on the wafer replicating the field nonuniformity of the electrostatic field generated by the mask-membrane charging. If the incident electron is deflected at an angle  $\Delta\alpha_{\text{after}} < \alpha_0$  after the mask, it will cause a pattern placement error on the wafer. In average  $\Delta\alpha_{\text{above}} \approx \Delta\alpha_{\text{after}} \approx \Delta\alpha_{\text{tot}}/2$  where  $\Delta\alpha_{\text{tot}}$  is the total angle of deflection at the mask. Obviously, the maximum deflection,  $\Delta\alpha_{\text{max}}$ , that an incident electron can experience will be at the edge of the subfield; in the case considered ( $E_0 = 100$  keV,  $\epsilon_{\text{SiN}_x} = 7$ ,  $a = 0.5$  mm),  $\Delta\alpha_{\text{max}} \approx 50 t_m q$ .

Any deviation of an incident electron from its original (unperturbed) direction after the mask at an angle  $\Delta\alpha_{\text{after}} \approx \Delta\alpha/2 < \alpha_0$ , will cause a trajectory displacement at the wafer plane in the SCALPEL tool,  $\Delta x_w$ . Because the projection lens system in SCALPEL transfers the mask pattern onto the wafer with  $4\times$  demagnification,<sup>2</sup> any shift at the mask of a ray carrying information will be also demagnified;  $\Delta x_w = \Delta x_{\text{mask}}/4$ . The shift at the mask,  $\Delta x_{\text{mask}}$ , has been evaluated by numerically calculating the electron trajectories above and after the mask and then defining the coordinates of crossings of their asymptotes with the membrane surface.<sup>2</sup> As a result we have found  $\Delta x_{w-\text{max}} \approx 2.5 \times 10^{-10} q$  ( $\Delta x_{w-\text{max}} \approx 0.55 \times 10^{-4} \Delta\alpha$ ).

#### IV. RESULTS AND CONCLUSION

As was shown in Sec. II, depositing a thin (undoped) poly-Si or *a*:Si on top of a dielectric membrane provides only limited improvement in the suppression of the membrane charging effect; in this case the advantage of having a TSCL is not fully realized because  $I_s < I_2$ . Maximum suppression of the effect can be achieved if the TSCL is doped beyond a certain level,  $N_d \geq N_{d-\text{min}}$ , making  $I_s \geq I_2$ . In this case, the charging effect of the membrane stack (limited by the flux  $I_2$ ) is described by Eqs. (2.8)–(2.10) and can be evaluated straightforwardly.

The results of steady state charging effect in the SCALPEL mask membranes with a 10 nm TSCL of B doped poly-Si are presented in Fig. 3 and Table II. For comparison, the results for the charging of currently used SCALPEL mask membranes without any TSCL are presented as well (Refs. 1 and 2). One can see that a 10 nm B doped poly-Si film deposited on top of  $\text{SiN}_x$  membrane will effectively reduce the charging of SCALPEL mask membranes keeping its effect within the acceptable limits for tool performance even in a worst case scenario of steady state charging. One can also see (Table II) that in this case the deflection angle of an incident electron caused by the membrane charging is much smaller than the SCALPEL aperture size independent of the exposure dose. Therefore, a TSCL helps to eliminate any possibility of illumination nonuniformity built up on the wafer discussed in Sec. III. The only impact of the charging of the membrane with a TSCL is limited to a negligible

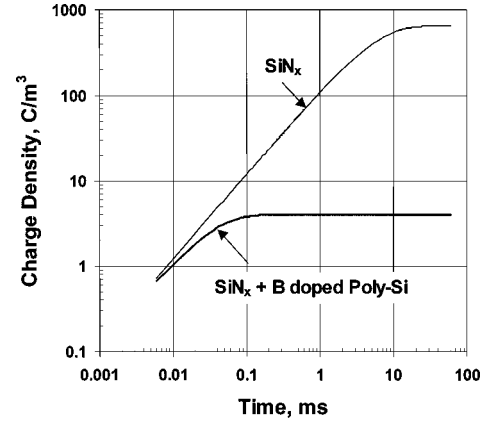


FIG. 3. Charging effect of SCALPEL mask membranes without and with TSCL;  $E_0 = 100$  keV,  $I = 100 \mu\text{A}$ ,  $t_s = 10$  nm,  $t_m = 100$  nm,  $\mu_{\text{SiN}_x} = 5 \times 10^{-6} \text{ m}^2/(\text{V s})$ ,  $\mu_{\text{P-Si}} = \times 10^{-3} \text{ m}^2/(\text{V s})$ .

(about 1 nm) image placement error in the wafer plane. Note, when the TSCL doping level is above  $N_{\text{min}}$  [given by Eq. (2.7)], the membrane charging dynamics is entirely defined by the hole flux limitations in the membrane [Eqs. (2.8)–(2.10)]. Therefore, membranes with TSCL doped to a certain level have the advantage of both effectively suppressing the charging effect and making it pattern independent.

This simple modification of the mask-membrane structure will not alter the mask contrast (defined by the scatterer thickness only)<sup>11</sup> at all and will have a negligible impact on the membrane transmission; the addition of 10 nm Si on top of 1000 Å  $\text{SiN}_x$  would cause less than a 10% decrease of the  $\text{SiN}_x$  membrane transmission [see Fig. 3(a) of Ref. 11], reducing the total transmission by only 1% (14% instead of 15%).

The required structure can be simply generated by regulating the gas flows in the low-pressure chemical vapor deposition process to produce a thin final layer of *a*:Si or poly-Si. The required level of the TSCL doping,  $N_d \geq N_{d-\text{min}} \approx 0.75 \times 10^{21} \text{ m}^{-3}$  (for poly-Si), is rather low. The TSCL can therefore be doped *in situ* during deposition or after deposition by diffusion or implantation.<sup>7</sup> A comparison of the three doping processes shows that the major differences are lower resistivity for diffusion, lower dopant concentration for implantation, and lower mobility for *in situ* doping.<sup>7</sup> Due to the moderate doping levels required, *in situ* doping during deposition seems to be the most appropriate in the case considered because of (i) simplicity, (ii) a large increase in the deposition

TABLE II. Steady state charging of the SCALPEL  $\text{SiN}_x$  mask membranes without and with the TSCL (B doped poly-Si) and its effect on a 100 keV beam electron incident at the edge of the  $1 \times 1 \text{ mm}^2$  exposed area where the electrostatic field of the charge accumulated in the membrane has maximal strength. The parameter values are the same as in Fig. 3.

Top conductive layer	$q_s$ (C/m <sup>3</sup> )	$\tau_s$ (ms)	$\Delta\alpha_{\text{max}}$ (mrad)	$\Delta x_{w-\text{max}}$ (nm)
None	$4.55 \times 10^2$	5.4	2.2	$10^3$
B doped poly-Si <sup>a</sup>	4.0	0.03	0.02	1.0

<sup>a</sup>Boron doped poly-Si with density of holes  $N_d \geq N_{d-\text{min}} \approx 0.75 \times 10^{21} \text{ m}^{-3}$ .

rate caused by adding of diborane,  $B_2H_6$ , to the reactants, (iii) columnar Si structure (with a constant low resistivity) formed at relatively low deposition temperatures, 580 °C and higher, and (iv) higher density and distribution uniformity of boron across the surface poly-Si layer.<sup>7</sup>

In conclusion, it should be mentioned that in the practice there might be no need to deposit a TSCL on top of mask membrane; the charge flux driven by the  $E_z$  component of the electrostatic field through the membrane thickness can also be transported via the semicontinuous metal pattern on the membrane. SCALPEL masks are expected to be mostly dark field, by an appropriate choice of resist tone. (A dark field mask has the advantage of reducing the space charge effects and making it less dependent on the pattern density.<sup>12</sup>) For instance, in application-specific integrated circuits (ASICs), static random access memories (SRAMs), and dynamic random access memories (DRAMs) the pattern density is about 10%, 40%, and 45%, respectively, for the gate level, and about 5% for the contact hole level. This will correspond to less than 50% open area in a SCALPEL mask if a negative tone resist is used for printing gates and a positive tone resist for printing contact holes. For a dark field SCALPEL mask the membrane charging will be defined by a flux that is, on average, less than  $I_2 \propto \sigma_{SiN_x} 4a^2$  but is still much larger than  $I_3 \propto \sigma_{SiN_x} 2at_m$ , which will keep the membrane charging at an acceptably low level.

## ACKNOWLEDGMENTS

This work was supported, in part, by International SEMATECH and DARPA under Contract No. MDA972-98-C-0007.

- <sup>1</sup>M. M. Mkrтчyan, A. Gasparyan, K. Mkhoyan, A. Liddle, and A. Novembre, *Microelectron. Eng.* **46**, 223 (1999).
- <sup>2</sup>M. M. Mkrтчyan, A. Gasparyan, K. Mkhoyan, A. Liddle, A. Novembre, and D. Muller, *SCALPEL Mask-Membrane Charging*, Bell Labs Technical Memorandum, BL011122-990120-13-TM (1999).
- <sup>3</sup>D. A. Muller and J. A. Liddle, *Electron Beam Radiation Damage in Silicon Nitride Membranes for SCALPEL Masks*, Bell Labs Technical Memorandum, BL111A-980204-011M, BL11122D-9802040-081M (1998).
- <sup>4</sup>W. Liu, J. Ingino, and R. F. Pease, *J. Vac. Sci. Technol. B* **13**, 1979 (1995).
- <sup>5</sup>S. Fijita and A. Sasaki, *J. Electrochem. Soc.* **132**, 398 (1985).
- <sup>6</sup>*CRC Handbook of Chemistry and Physics*, edited by D. R. Lide, 78th ed. (CRC, Cleveland, 1997).
- <sup>7</sup>S. M. Sze, *VLSI Technology*, 2nd ed. (McGraw-Hill, New York, 1988).
- <sup>8</sup>T. I. Kamins, *J. Appl. Phys.* **42**, 4357 (1971).
- <sup>9</sup>P. G. LeComber, D. I. Jones, and W. E. Spear, *Philos. Mag.* **35**, 1173 (1977).
- <sup>10</sup>J. Jang, S. C. Kim, D. B. Lee, and C. Lee, *Proceedings of the MRS Symposium* (Material Research Society, Pittsburgh, 1987), p. 565.
- <sup>11</sup>M. M. Mkrтчyan, J. A. Liddle, A. E. Novembre, W. K. Waskiewicz, G. P. Watson, L. R. Harriott, and D. Muller, *J. Vac. Sci. Technol. B* **16**, 3385 (1998).
- <sup>12</sup>S. T. Stanton, J. A. Liddle, W. K. Waskiewicz, and M. M. Mkrтчyan, *J. Vac. Sci. Technol. B*, these proceedings.